UNCLASSIFIED

AD

INFRARED DYE LASER STUDY

Final Report - Phase I

by
J. P. Webb
B. E. Plourde

September, 1972
Night Vision Laboratory
U. S. Army Electronics Command
Fort Belvoir, Virginia, 22060

Prepared by
EASTMAN KODAK COMPANY
Kodak Apparatus Division
901 Elmgrove Road
Rochester, N. Y. 14650

D D C

SEP 27 1972

B

Contract No. DAAK02-72-C-0012

Distribution Statement

Approved for public release; distribution unlimited

UNCLASSIFIED

Distribution Statement

Approved for public release; distribution unlimited.

DOCUMENT CONTROL DATA - R & D

(Security classification of title, body of abstract and indexing annotation must be entered when the overall report is classified)

1 ORIGINATING ACTIVITY (Corporate author)	2a. REPORT SECURITY CLASSIFICATION
Eastman Kodak Company Kodak Apparatus Division 901 Elmgrove Road Rochester, New York 14650	Unclassified
	2b. GROUP ---

3 REPORT TITLE

INFRARED DYE LASER STUDY

4 DESCRIPTIVE NOTES *(Type of report and inclusive dates)*

Final Report - Phase I, September 1971 to September 1972

5 AUTHOR(S) *(First name, middle initial, last name)*

Julian P. Webb
Bert E. Plourde

6 REPORT DATE	7a. TOTAL NO OF PAGES	7b. NO OF REFS
September 1972	74	9
8a CONTRACT OR GRANT NO DAAK02-72-C-0012	9a. ORIGINATOR'S REPORT NUMBER(S) ---	
b. PROJECT NO 1S663719DK70/08		
c.	9b OTHER REPORT NO(S) (Any other numbers that may be assigned this report) ---	
d.		

10 DISTRIBUTION STATEMENT

Approved for public release; distribution unlimited.

11 SUPPLEMENTARY NOTES ---	12 SPONSORING MILITARY ACTIVITY Night Vision Laboratory U. S. Army Electronics Command Fort Belvoir, Virginia, 22060

13 ABSTRACT Near infrared laser action has been demonstrated for 9 Kodak organic dyes, using a linear flash lamp for excitation. The spectral region covered by these 9 dyes extends from 850 nm to at least 960 nm, with no tuning attempted so far. Output is in the kilowatt and millijoule range. In comparison with DTTC, a polymethine dye that has recently been lased under excitation by an ultra fast coaxial flash lamp, the best laser dyes from this work have over 10 times more laser output when tested under identical conditions.

Recommended extensions to this work include procurement of larger amounts of lasing dyes for use in a flow system, further investigation of new dyes and solvents, development of a more reliable laser test facility to aid system optimization, and research to improve the spectral overlap between flash lamp output and dye absorption.

14 KEY WORDS	LINK A		LINK B		LINK C	
	ROLE	WT	ROLE	WT	ROLE	WT
Dye laser Infrared light source (850-960 nm) Flash lamp laser excitation						

UNCLASSIFIED

INFRARED DYE LASER STUDY

Final Report - Phase I

by
J. P. Webb
B. E. Plourde

September, 1972
Night Vision Laboratory
U. S. Army Electronics Command
Fort Belvoir, Virginia, 22060

Prepared by
EASTMAN KODAK COMPANY
Kodak Apparatus Division
901 Elmgrove Road
Rochester, N. Y. 14650

Contract No. DAAK02-72-C-0012

DA Project/Task No. 1S663719DK70/08

Distribution Statement

Approved for public release; distribution unlimited

UNCLASSIFIED

INFRARED DYE LASER STUDY

Final Report

Phase I

Summary

Near infrared laser action has been demonstrated for 9 Kodak organic dyes, using a linear flash la..p for excitation. The spectral region covered by these 9 dyes extends from 850 nm to at least 960 nm, with no tuning attempted so far. Output is in the kilowatt and millijoule range. In comparison with DTTC, a polymethine dye that has recently been lased under excitation by an ultra fast coaxial flash lamp (1, 2', the best laser dyes from this work have over 10 times more laser output when tested under identical conditions.

Recommended extensions to this work include procurement of larger amounts of lasing dyes for use in a flow system, further investigation of new dyes and solvents, development of a more reliable laser test facility to aid system optimization, and research to improve the spectral overlap between flash lamp output and dye absorption.

(1) G. Carboni, A. Dibene, C. Goroni, E. Polacco and G. Torelli, Lett. Al Novo Cimento 1, 979 (1971).

(2) A. Hirth, J. Faure & R. Schoenenberger, Compt. Rendus - Serie B 274, 747 (1972).

Forword

TABLE OF CONTENTS

LIST OF ILLUSTRATIONS AND TABLES

Illustrations

Tables

INFRARED DYE LASER STUDY

I. Introduction and Background

Introduction

This research was directed at finding organic dye solutions that would serve as convenient laser materials in the spectral region from 850 to 960 nanometers. Criteria for convenient operation include:

a) flash lamp pumpable

b) room temperature operable

c) optical quality of laser media easily achievable through use of liquid host

In meeting these goals we identified 9 proprietary Kodak dyes that exhibit laser action under flash lamp excitation in this spectral region.

The spectral range of interest is bounded by the long wavelength cut off of efficient photocathodes and by the extreme infrared limit of visual sensitivity. This spectral region is not richly endowed with laser active materials. Since organic dyes exist in great variety, it is reasonable to anticipate that some dyes should lase in this wavelength region (3).

An advantage in using flash lamps to excite dye lasers is that the natural pulse length ... ~ 1 μsec ... is the right duration for use in conjunction with gated image detectors. A dye laser,

---

(3) Near infrared laser emission has already been observed from a variety of polymethine dyes under giant pulse ruby laser excitation:
(i) Y. Miyazoe & M. Maeda, Appl. Phys. Lett 12, 206 (1968).
(ii) Y. Miyazoe & M. Maeda, Opto-electronics 1, 227 (1970).

however, has relatively low efficiency in utilizing the input electrical energy to generate infrared output.

While dye lasers have been described in many excellent review articles (4, 5, 6, 7), a brief description is presented here both for completeness and to standardize on notation to be used later.

Organic Dye Lasers

Dye lasers use an organic dye dissolved at low concentration about 10^{-4} mole/liter) in a suitable liquid solvent. The dye solution is contained in a transparent cell with end windows of high optical quality and located in an resonant cavity formed by a pair of mirrors that are carefully aligned perpendicular to the optical axis of the cell. Axial radiation trapped between the mirrors will reflect back upon itself and retraverse the active medium many times. A population inversion is induced in the laser active material so that there are more molecules in a higher energy level than a lower one. Trapped radiation with a frequency ν equal to this energy level difference/h, will be amplified by stimulated emission during each pass through the active region. The population inversion is essential for amplification, since the cross sections for stimulated emission and absorption are equal.

---

(4) P. Sorokin, J. Lankard, V. Moruzzi, and E. Hammond,
J. Chem. Phys. 48, 4726 (1968).

(5) B. Snavely, Proc. IEEE 57, 1374 (1969).

(6) O. Peterson, J. Webb, W. McColgin and J. Eberly,
J. A. P. 42, 1917 (1971).

(7) M. Bass, T. Deutsch and M. Weber, Dye Lasers appearing in
Lasers Vol 3, p. 269, ed Levine & DeMaria, (Marcel Dekker Inc.
New York, 1971).

Since the process of stimulated emission requires that each secondary photon emitted in a stimulated transition have the same wavelength, direction of propagation, and phase as the triggering photon, stimulated emission funnels energy preferentially into the "trapped radiation" mode. The source of this energy is the excitation that "pumps" the laser-active material to its excited state producing the necessary population inversion. A dye laser is thus a form of transducer, converting incoherent, polychromatic, non-directional excitation radiation from the flash lamp into coherent, collimated, monochromatic laser output radiation at a wavelength determined by the laser active material. Laser threshold occurs when the photon gain from stimulated emission exceeds the losses from mirror transmission, off-axis fresnel reflections, fresnel diffraction, scattering within the cavity, and absorption at the laser wavelength.

The organic dye in the solution is the laser active molecule. Solvent molecules, in principle, serve merely as a dilutant host. In practice, however, the solvent is not an inert host, and fluorescence yields from a dye depend on the solvent for reasons that are not well understood. Optical loss mechanisms related to thermal inhomogeneities and bubble formation can be different for each solvent.

In a dye molecule, it is useful to think of the conjugated chain comprising the chromophore of a dye as a core plus a π electron cloud. Neglecting the core of nuclei, inner-shell and σ bonding

3

electrons, the π electron cloud consists of electrons from overlapping π orbitals of adjacent atoms; these overlapping π orbitals form, molecule-sized wave functions that are spread over most of the molecule. The electrons in these π wave functions are not tightly bound and are the electrons involved in near-ultraviolet, visible, and near-infrared optical transitions.

To an extent the π electrons can be thought of as a one-dimensional gas of free electrons. Thus, a longer chromophore, i.e. a longer conjugated chain with its associated π electrons, is a longer "box" for the π electron wave functions, and the energy-level spacing is correspondingly reduced. When comparing two similar dyes, absorption and fluorescence will occur at longer wavelengths for the dye with the longer chromophore.

Because the molecule is large and has many bonds and internal degrees of freedom, there are many opportunities for vibration and rotation along different bonds, and the simple "electron-in-a-box" energy levels are split into many, virtually continuous levels. Figure 1 is a schematic representation of the π- orbital energy levels of a dye molecule. Each submanifold, denoted by S_i and T_i, is a single "electron-in-a-box" level, and each is split into a continuum of vibrational levels (heavy lines) and rotational levels. Excited electronic states (1, 2, etc.) can be either singlet or triplet, with triplet submanifolds usually slightly lower in
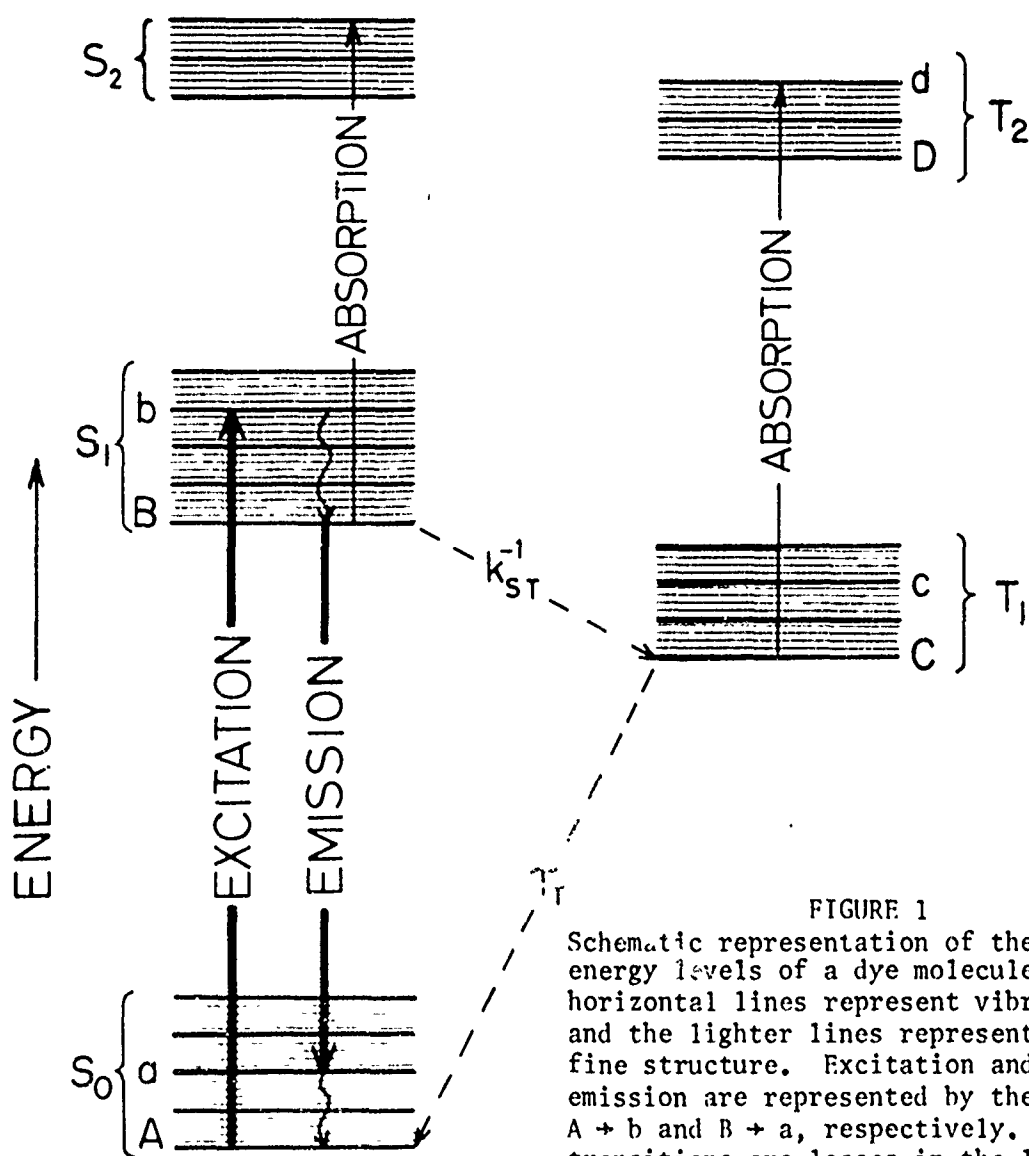
4

SINGLET
STATES

TRIPLET
STATES

FIGURE 1

Schematic representation of the π-orbital
energy levels of a dye molecule. The heavy
horizontal lines represent vibrational states
and the lighter lines represent rotational
fine structure. Excitation and laser
emission are represented by the transition
A → b and B → a, respectively. Other
transitions are losses in the laser process.

5

energy than the corresponding singlet levels. Excitation of the
first excited singlet state by absorption of pump light and
spontaneous or stimulated emission are indicated by heavy, vertical
arrows.

Electric dipole radiative transitions occur only between
states of the same multiplicity, i. e., singlet-to-singlet or
triplet-to-triplet. Radiative transitions other than electric-dipole
are too improbable to compete with other relaxation process, and
may be neglected.

Insight into dye laser operation can be gained by following
the dye through an absorption and emission cycle. Initially, most of
the dye molecules are in thermal equilibrium in vibrational or
rotational states at or near level A in the electronic ground singlet
manifold S_0. In accordance with the Franck-Condon principle, the
most probable absorption is between these A levels in S_0 and
rotationally and vibrationally excited states b in the first excited
electronic manifold S_1. (A-B transitions are much less probable.)
These excited molecules can relax by several routes. The most
rapid relaxation process is thermal equilibration within S_1 to
vibrational and rotational states near B. Since thermal equilibration
occurs on a picosecond time scale, the bulk of the excited dye
molecules end up in B, i. e. in the lowest vibrational and rotational

states of the first electronic excited manifold.

There are relaxation processes from the S_1 manifold.

These include spontaneous fluorescence, radiationless "internal conversion" from S_1 to S_0, and radiationless "intersystem crossing" from S_1 to the triplet manifold T_1 at a rate constant k_{ST}. Laser action occurs through amplification by stimulated emission of naturally occurring, spontaneous emission from level B back to the ground electronic manifold. Once more, the most probable transition is to an excited vibrational state, a, in S_0, rather than to the ground vibrational state A. Thermal equilibration occurs very rapidly from these laser-terminus, a states, and the population of dye molecules in the S_0 manifold maintains itself in a Boltzmann distribution, i. e., with only the lowest levels around A significantly populated.

This very fast thermal equilibration in the ground electronic manifold means that the molecular terminal states of the laser will always be emptied. This rapid emptying of the states means that population inversion, between a-B levels, is achieved relatively easily.

Laser threshold occurs when photon gains from stimulated emission exceeds photon losses at the potential laser wavelength. In addition to extrinsic losses such as imperfect mirror reflectivity and scattering, loss mechanisms intrinsic to the dye are crucial to laser operation, and ultimately determine the suitability of a dye for laser use. These intrinsic loss

7

mechanisms include low quantum yield and absorption by the dye itself of fluorescent emission at the laser wavelength. Self absorption can occur, in principle, from the ground electronic manifold (S_0) to S_1, from the first excited electronic manifold (S_1) to higher electronic excited manifolds ($S_2, \cdots$), and from the lowest triplet manifold (T_1) to higher excited triplet manifolds ($T_2, \cdots$). From first order perturbation theory, the rate of absorption of photons of energy $E = h\nu$ by a molecule in initial state $|i\rangle$ of energy E_i is given by the expression

$$W_{i \to f} = \frac{(2\pi)^2}{\hbar} \left| \langle f | V | i \rangle \right|^2 \rho(E_f = E_i + h\nu) \qquad (1)$$

where V is the perturbing term in the Hamiltonian responsible for the transition, $|f\rangle$ is the final state of energy E_f and $\rho(E_f)$ is the density of final states. For the most important case of electric dipole coupling,

$$\left| \langle f | V | i \rangle \right|^2 = \frac{h\nu}{2} \frac{N}{v\eta^2} \left| \left(\underset{\sim}{u}_{if} \cdot \left(\underset{\sim}{e} \right) \right) \right|^2 \qquad (2)$$

where N is the number of photons in the laser mode considered and hence is proportional to radiation intensity in the cavity, ν and $\underset{\sim}{e}$ are the frequency and polarization vector of the mode, v is the cavity mode volume, $\underset{\sim}{u}_{if}$ is the dipole transition matrix element, and η is the index of refraction of the medium in which the transitions are occurring.[6]

(6) O. Peterson, J. Webb, W. McColgin and J. Eberly, J. A. P. 42, 1917 (1971).

Multiplying the molecular absorption rate, $W_{f \leftarrow i}$
by the number of molecules N_i in the initial state, and then
summing $N_i \, W_{f \leftarrow i}$ over all pairs of initial and final states whose
energy difference $E_f - E_i = h\nu$ gives the total self absorption
for light at the potential laser frequency ν. Self absorption is
thus proportional to the number of atoms in a potential initial
state, to the density of states at $E_f = E_i + h\nu$, and to the
dipole matrix element (squared).

One obvious source of self absorption is from states
around a (the laser terminus level) in S_o. The matrix element for
absorption from a to B is the same as for stimulated emission, and
is large; the density of states at B is also large. The rapid
thermal equilibration within the electronic manifold insures that
the population of these a states will be relatively low, but
always finite, due to the high energy tail of the Boltzmann distribution.
For the laser dye DTTC, for example,

$$\exp\left(-\frac{E_a - E_A}{kT}\right) \approx$$

$$\approx \exp\left[-\frac{(E_a - E_A) + (E_b - E_B)}{2kT}\right] = \exp\left[-\frac{h\nu_{abs\ max} - h\nu_{laser}}{2kT}\right]$$

is estimated to lie between .01 and .02, assuming $(E_a - E_A) \approx (E_b - E_B)$.
Since the excited state (S_1) population of a flashlamp-pumped dye laser is
only a few percent, this effect is a large loss. Self absorption from S_0 can

9

be estimated qualitatively from steady state absorption and fluorescence spectra. The larger the Stokes shift (separation between absorption and fluorescence maxima), the lower the $S_0 - S_1$ self absorption will be.

Self-absorption between the substantial excited state population at B in S_1 and S_2 depends upon the density of states at an energetically appropriate S_2 level and the magnitude of the matrix elements connecting these states with low lying states is S_1. These factors can certainly vary from dye to dye. Since stimulated emission and $S_1 - S_2$ absorption processes compete for the same S_1 molecules, $S_1 - S_2$ self-absorption can completely quench laser action if

$\left| < S_2 \left| V \right| S_1 > \right|^2 \rho(E_2 = E_1 + hv)$ is greater than $\left| < S_0 \left| V \right| S_1 > \right|^2 \rho (E_0 = E_1 - hv)$. Since $S_1 - S_2$ absorption is very difficult to measure as is triplet-triplet absorption, we have avoided the whole issue by simply trying dyes in a laser test facility. If the dyes lase, $S_1 - S_2$ absorption is presumably small.

Intersystem crossing to the triplet manifold is particularly deleterious because of the long lifetime τ_T of this metastable state. Dye molecules continue to accumulate in T_1, where they are not only lost to the laser emission process, but-- far worse-- where they can absorb photons from the potential laser mode by being promoted to excited triplet states in T_2. Triplet-triplet absorption is a severe enough problem in general to limit

10

dye laser operation to the restricted class of dyes having low triplet yield (small k_{ST}), or to fast systems where the time for excitation peaks in the order of k_{ST}^{-1}, or to systems with triplet quencher additives that reduce τ_T to the order of k_{ST}^{-1}. Very fast excitation generally means pumping by a Q-spoiled laser, or by special fast flash lamp.

The growth of intensity I of a laser beam as it propagates through the excited dye can be described by a Beer's law gain equation of the form

$$\frac{dI}{dl} = GI \tag{3}$$

The gain coefficient G is given by

$$G = n^* \sigma_g(\nu) - n_0 \sigma_S(\nu) - n^* \sigma_{SS}(\nu) - n_T \sigma_T(\nu) - r \tag{4}$$

where n_0, n^* and n_T are the number densities of singlet ground-state, singlet excited-state, and triplet-state molecules, respectively; $\sigma_S(\nu)$, $\sigma_{SS}(\nu)$ and $\sigma_T(\nu)$ are the singlet-singlet $(S_0 - S_1)$, excited singlet-singlet $(S_1 - S_2)$ and triplet-triplet molecular absorption cross sections; and r is the average extrinsic loss per unit length of dye, incorporating all intracavity losses except the dye absorbances. The average intracavity loss due to mirror reflectivities R_1 and R_2, for example, is given by $r = -\ln(R_1 R_2)/2\ell$, where ℓ is the length of the dye cell (5,6). The stimulated emission cross section $\sigma_g(\nu)$ can be shown (5,6) to be

(5) B. Snavely, Proc. IEEE 57, 1374 (1969).

(6) O. Peterson, J. Webb, W. McColgin and J. Eberly, J. A. P. 42, 1917 (1971).

$$\sigma_g(\nu) = c^2 g(\nu)/8\pi\nu^2 \tau_S n^2 \qquad (5)$$

τ_S is the spontaneous singlet decay time, ν and c are the frequency
and velocity of light in vacuum, n is the index of refraction of
the solution, and $g(\nu)$ is the fluorescence line shape normalized
so that $\int_0^{\infty} g(\nu)d\nu$ equals the quantum yield ϕ. Positive gain
results solely from the $n^*\sigma_g(\nu)$ term in (4); all other terms
represent losses.

The total dye concentration n is equal to the sum
of n_0, n^* and n_T. One can assume that n^* is spatially
uniform, an approximation that corresponds experimentally to a
cylindrical dye cell uniformly pumped by a parallel flash lamp
imaged in the cell and operated near threshold where I is low
enough so stimulated processes do not change n^* and I·significantly
over the length of the cell. Laser threshold, in particular, is
defined by G = 0, and the threshold inversion is trivially derived
from Equation 4.

$$\left(\frac{n^*}{n}\right)_{G=0} = \frac{\sigma_S + r/n}{\sigma_g - \sigma_{SS} + \sigma_S - (\sigma_T - \sigma_S)\, n_T/n^*} \qquad (6)$$

Equation 6 is evaluated at the wavelength of laser emission.
This will occur at some wavelength greater than that of the
singlet-singlet absorption maximum, where generally

$\sigma_S(\nu) \ll \sigma_g(\nu)$ and $\sigma_T(\nu) \lesssim \sigma_g(\nu)$.

Since the triplet state is populated at a rate equal to $k_{ST}n^*$, and spontaneously empties at a rate equal to n_T/τ_T, n_T can be expressed in terms of n^*, k_{ST} and τ_T. The ratio of triplets to excited singlets, $n_T(t)/n^*(t)$, depends upon the time history of excitation, but is of the order of $k_{ST}T$ where $T = \tau_T t/ (\tau_T + t)$ and t is the time since inception of excitation.

The importance of fast excitation is obvious from equations (6) and (4). From (6), short time excitation ($t < \tau_T$) is desirable to reduce the triplet build up and hence the threshold inversion $(n^*/_n)_{G=0}$. We wish to maximize n^* in equation (4). Since n^* increases with the excitation intensity (at least until $(n^*/_n)$ is fixed at the threshold inversion $(n^*/_n)_{G=0}$ by the onset of laser action), the highest pumping intensity is desired. This implies dissipating the maximum excitation energy in the shortest time.

The infrared emitting dyes are molecules with a molecular weight of 600 to 1000. This size aids in obtaining the close energy level spacing necessary for infrared optical transitions. Because of their size, these molecules are relatively nonrigid and unstable; nonrigidity leads to non-radiative internal conversion and lower quantum yields. Efficient laser operation depends on a balance of molecular gain $n^*\sigma_g$, extrinsic losses, and losses intrinsic to the dyes.

II. Outline of Experiments

This investigation sought organic dye solutions that would exhibit laser action in the spectral region from 850 to 960 nanometers. The dyes to be screened had been developed previously in the Kodak Research Laboratories for other purposes and existed in milligram quantities.

The goal of the project was to avoid a major research program by identification of existing dyes that exhibit laser action in the near infrared. The program included careful selection of promising dyes from the Kodak dye files, construction of a dye laser test facility, demonstration of infrared laser action, and measurement of output power and wavelength. Data derived from these experiments would identify promising families of dyes, important structural elements of dyes, and complementary solvents. These data would prove helpful in learning the effects on laser action of different dye and solvent structures.

Chemists in the Kodak Research Laboratories initially screened our dye files for promising dyes. Based on the length of chromophore and the known effects of substituent groups, over thirty potential candidates were identified. Spectral absorption and fluorescence of these dyes were measured. About twenty of these dyes showed substantial fluorescence in the 850 to 960 nanometers region. Twenty-two dyes that exhibited the greatest fluorescence

in the 850 to 960 nanometers region were submitted for testing in the laser facility. Of the twenty-two, eighteen were sufficiently distinct from one another in structure to qualify as representatives of different dye "families".

Two laser test facilities were constructed as described in Section III. The first employed a fast coaxial xenon flash lamp; the second facility used a brighter but slower, low pressure air discharge in an ablating quartz tube. Because dye quantities were limited, only enough dye solution was mixed to fill the dye cell. Thermal equilibration was achieved by waiting 10 minutes after syringing the dye solution or solvent into the cell.

The coaxial lamp was purchased from Candela Corp. and gave a rise time of ~0.3 μsec. It was hoped that this time would be fast enough to minimize triplet-triplet absorption. Eight Kodak dyes were tested for laser action with this lamp, and no laser action was observed. Following these tests, the brighter but slower ablating lamp was used. At this point the importance of solvent effects was discovered through the fluorescence yield experiments described below. Tests with the ablating lamp generally used dyes in solvents that enhanced fluorescence, and laser action was observed with 9 dyes plus Kodak DTTC. Twenty dyes in DMSO were tried with the new lamp which previously had been tried with other solvents in the coaxial lamp. Two of these dyes lased in DMSO.

Laser output was detected with a fast silicon PIN photo diode with 0.2 mm^2 active area. The diode was placed on the laser axis and shielded by a filter passing only infrared radiation in order to reduce background noise. Since the detector saturated between 100 and 200 watts/cm^2, Inconel neutral density filters were added when testing the more efficient laser dyes.

Because the detector area was too small to intercept the whole laser beam, output power was measured by placing an opal glass diffuser of 4mm thickness 9 cm in front of the photo detector. Estimates of laser power were made from the detector-target geometry assuming the opal was a perfect diffuser.

The spectral band where laser emission occurred was measured using a Bausch & Lomb 1 1/2 meter grating spectrograph and Kodak High Speed Infrared Film 2481 (ESTAR Base). The sensitivity of this film was down from the peak value by two orders of magnitude at 940 nanometers, thus lasing wavelengths longer than 940 nanometers could be determined only for particularly energetic dyes.

Relative fluorescence yields of dyes were measured in many solvents. Flat bottomed vials containing 10^{-4}M dye solutions were excited from below by the ablating flash lamp used in the laser test program. A fiber optics probe collected fluorescence from the side of a layer of dye centered about 4mm above the bottom of the vial. Output from the probe was filtered to remove

16

radiation shorter than 700 nanometers wavelength and was detected

with our silicon PIN photodiode. The filter was removed for tests

on rhodamine 6G. For a given series of fluorescence measurements,

vials of dye were interchanged in a holder fastened

adjacent to the flash lamp in a manner that preserved the geometry

between probe, detector, and dye sample. The relative geometry of

components changed between fluorescence runs, but changes in

fluorescence yield resulting from this effect could be renormalized

by comparing fluorescence from a common standard dye (DTTC).

There are three advantages to this simple testing scheme:

(1) The test has permitted us to quickly measure the
relative fluorescence yields of many combinations
of dye and solvent.

(2) The fluorescence yield is measured on the same
microsecond time scale that is relevant to laser
action. Since cis-to-trans-to-cis isomerization
in the excited state may well reduce the peak
fluorescence yield while spreading the total
fluorescence yield out in time, it is advantageous
to resolve the peak fluorescence amplitude.

(3) It is important to measure the peak fluorescence
when the dye is excited by the short wavelengths
of the flash lamp used in the laser test facility.

The relative fluorescence yields are proportional to the product of

n^*, the quantum yield and the spontaneous fluorescence rate $1/\tau_S$

for the dyes. The quantity n^* is the excited state population

generated by the flash lamp used to excite the laser. These

relative fluorescence yields are essentially proportional to the positive

gain term, $n^*\sigma_g$ of the laser pumped by the same flash lamp.

17

In addition, this scheme can easily be adapted for measuring the relative importance of pumping by near infrared light in comparison to pumping across a wide spectrum. The feasibility of these comparative measurements was verified for 3 Kodak dyes. This kind of measurement would be an essential pre-requisite for any future work aimed at improving the coupling efficiency between flash lamp and infrared dye by using intermediate fluorescent dye solutions that convert the flash radiation to more effective longer wavelengths.

Although a useful test, the fluorescence measurements are crude in that only total output is measured with no spectral resolution of the fluorescence. Furthermore, equi-molar solutions were used for all dyes rather than solutions with equal penetration depths. The glass vials filter the short ultraviolet from the pumping light and the bottoms of the vials are of low optical quality, causing some variation in focussing the pump light into the dye volume viewed by the fiber optics probe. Finally, the fluorescence yields are simply the photo diode output signal uncorrected for the spectral sensitivity of the detector. The effects of penetration depth and cell filtering were investigated by varying concentrations of two dyes over ranges of 10X and 20X and by substituting quartz cells for glass when testing 5 dyes.

Quantitative changes in fluorescence yield induced by these changes

were not large, and do not change the qualitative picture that emerged

from the fluorescence yield measurements. Spectral resolution of the

fluorescence could not be accomplished with available time and

equipment.

It is important to investigate the stability of the dyes

under the intense, ultraviolet-rich pumping necessary to reach threshold

population inversion levels. In particular we wanted to investigate

whether absorption from long-lived photo bi-products would quench

subsequent laser action in the same dye solution. It seems that

these dyes degrade under intense flash lamp excitation, since we

observed visible bleaching and decreasing laser output when the

same 2 cm^3 charge of dye solution was lased several times. This

degradation is expected in a small sample, but the critical question

is whether or not absorption from photo degradation products would

quench subsequent lasing. We needed to know whether a circulating

dye solution in a laser with a large dye reservoir and flow system

would slowly degrade under repetitive use, or whether it would be

quickly poisoned. Since it is difficult to measure changes in

transmission from 0.997 to 0.994 and since laser threshold gain

is critically sensitive to intrinsic loss, the best test for the

production of poisoning absorbers was to lase a 2 cm^3 charge of

dye solution repetitively (letting it thermally equilibrate between shots) until lasing ceased. While general degradation can not be separated from photo-product poisoning, single shot lasing is certainly suggestive of poisoning, while a long series of successive lases implies both very low poisoning and less rapid degradation.

III. Apparatus

Three experimental apparatus were used to obtain the measurements described in Section II. These configurations were a coaxial fast flashlamp laser, a laser incorporating a linear ablating flashlamp, and a fluorometer employing the ablating lamp.

The laser system using the coaxial fast flashlamp is shown in Figure 2 where the following components are designated:

L - Helium-neon alignment laser, Metrologic ML 310

S - Beam Steerer, Oriel Model 6650

M_1, M_2 - Planar infrared mirrors, coated by Laser Energy Inc. in gimbal mounts, Lansing Model 10.203

W - Windows, antireflection coated by Laser Energy Inc.

F.L./D.C. - Coaxial flashlamp surrounding fused quartz dye cell (Furomoto design), 1 cm ID x ~ 19 cm long (14 cm pumped)

C - Capacitor for flashlamp energy storage; 25KV, 0.3 µf.

S.G. - Triggered spark gap

H.V. - High voltage power supply, Universal Voltronics BAN 32-5.5

T - Trigger circuitry for spark gap

B.S. - Beamsplitter

Sp - Spectrograph, B. & L. 1 1/2 meter grating instrument covering 850 to 1250 nm in first order spectrum

F - IR passing filter (10% Trans. at 690 nm - 90% Trans. at 750 nm)

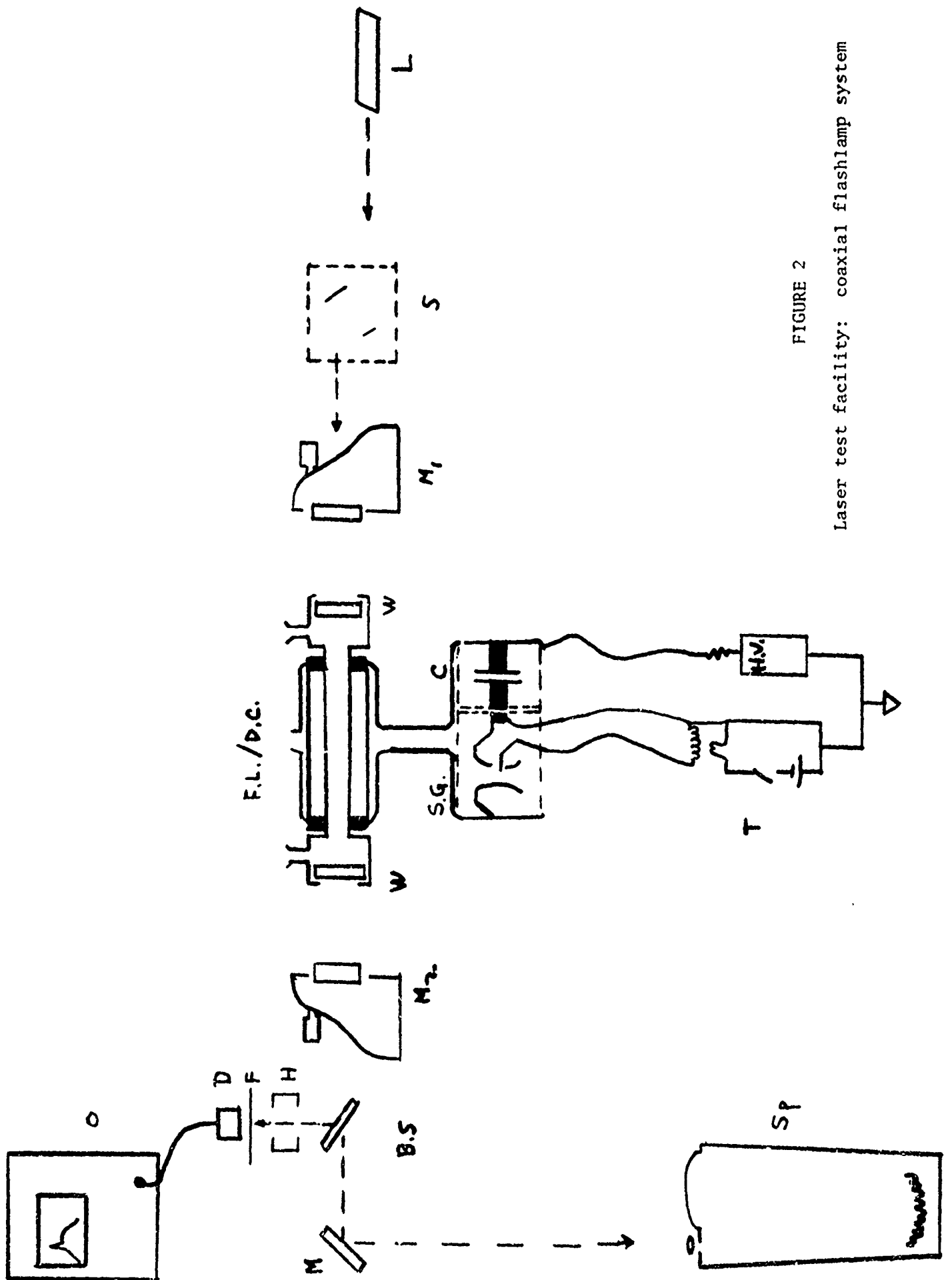D - Detector, Tropel 330, Silicon PIN photo diode

FIGURE 2

Laser test facility: coaxial flashlamp system

H - Misc. filter holder

O - Oscilloscope

The driving capacitor can store a maximum energy of
about 100 joules. However, the flashlamp output saturates at an
input energy of about 60 joules. The laser threshold value for
rhodamine 6G is 20 joules in this system used with mirrors of 90%
reflectivity at 580 nm. In this configuration the flashlamp has
a rise time of about 300 nsec.

Schlieren grade fused quartz windows, antireflection
coated at 930 ± 30 nm, contain the dye in the cell. The dye cell
is located in an optical cavity which is determined by one of two
sets of plane parallel mirrors. The mirrors of one set have a
99% to 97% reflectivity in the 850-900 nm spectral region, while
the other set has a 99% to 95% reflectivity in the 900-960 nm
spectral region. Both mirrors of the cavity are identical.

A helium-neon laser, adjustable beam steerer, and
apertures are used to align the cavity mirrors and the dye cell.
The optical axis is perpendicular to the cell windows which are
antireflection coated. This coating is used rather than using
windows set at Brewster's angle, so that solvents with differing
indices of refraction can be interchanged without need for drastic
realignment of the optical elements. The mirrors are held in
Lansing gimbal mounts. The flashlamp and dye cell, mirror mounts,
alignment laser, and beam steerer are all rigidly mounted to

an optical bench. In order to test scarce dyes, we have minimized

the needed volume of dye solution by using only enough dye solution

to fill the cell itself. A circulating system was not used, but

rather, rinsing cooling, and thermal equilibration between shots

were accomplished by syringing solvents in and out of the cell,

and by waiting between flashes.

Laser emission from candidate dye solutions was directed

through an infrared passing filter to reduce background radiation,

and then detected with a fast PIN photo diode and a Tektronix

549 oscilloscope. The spectral distribution of the output was

determined on a 1.5 meter Bausch and Lomb grating spectrograph

using infrared sensitive film. The spectrograph has a dispersion

of 20 nm/cm.

The laser system incorporating the linear, ablating

flashlamp is arranged as shown in Figure 3 where the following

components are designated:

L - Helium-neon alignment laser, Metrologic ML 310

S - Beam steerer, Oriel Model 6650

M_1, M_2 - Planar infrared mirrors, coated by Laser Energy Inc. in gimbal mounts, Lansing Model 10.203, 40 cm separation

D.C. - Dye cell, $\sim$ 3mm ID x 14 cm long of fused quartz

F.L. - Linear, ablating quartz flashlamp, 3mm ID x 15 cm long

R.C. - Diffusely reflecting cavity

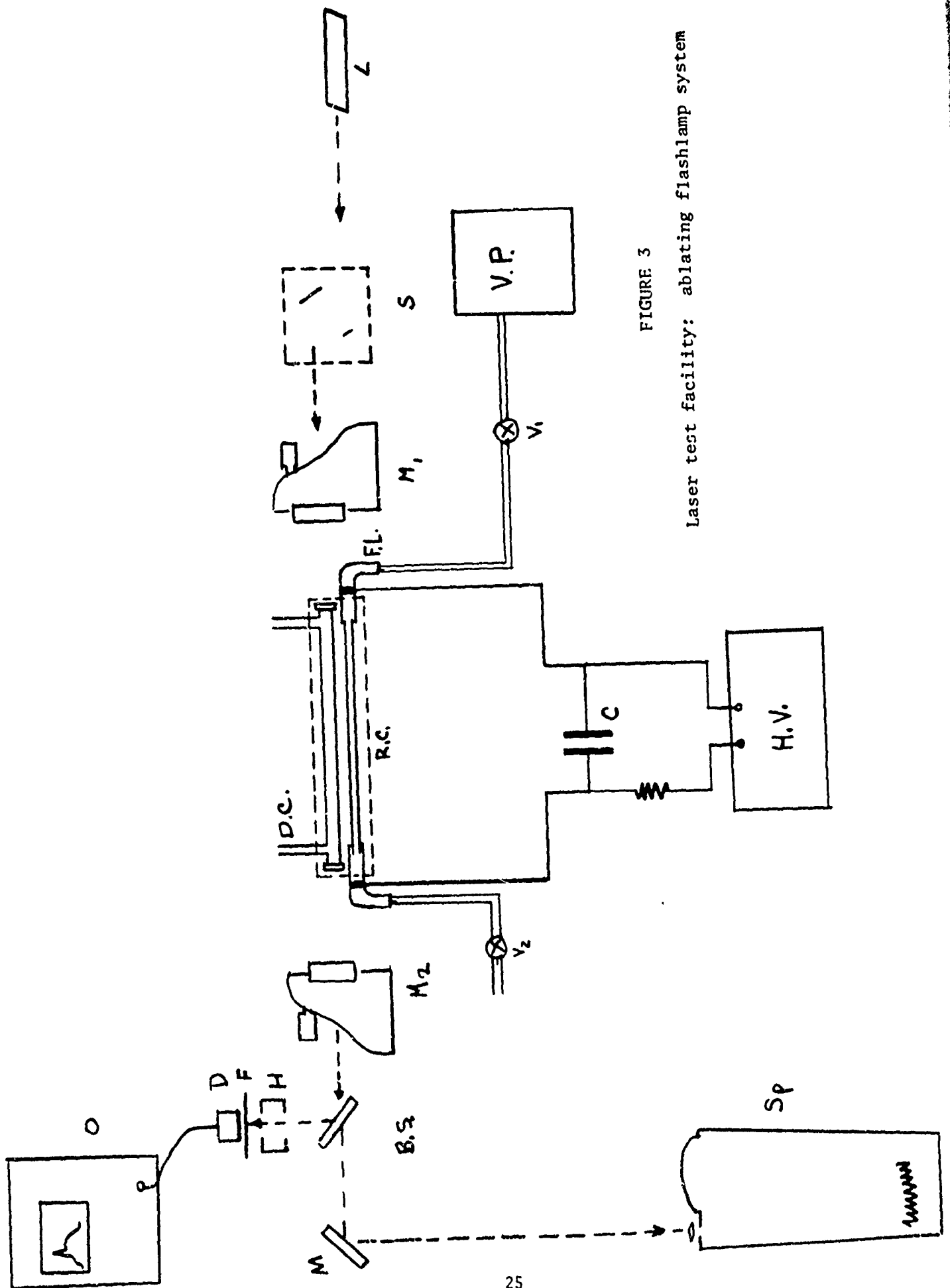C - Capacitor for flashlamp energy storage (20KV, 1 μf)

FIGURE 3

Laser test facility: ablating flashlamp system

H.V. - High voltage power supply

V.P. - Vacuum pump

V_1 - Main value

V_2 - Trigger value

F - Infrared passing filter

H - Filter holder

B.S. - Beamsplitter

Sp - Spectrograph, Bausch & Lomb 1 1/2 m grating
instrument covering 850 to 1250 nm in first
order spectrum

D - Detector, Tropel 330 Photo Diode

O - Oscilloscope, Tektronix 549

The light output from this lamp does not saturate until
the energy input exceeds 162 joules and has a rise time of about 700
nsec. The laser threshold value for rhodamine 6G is 23 joules in
this system using the same mirrors as before.

The dye sample is placed in a quartz tube of 2-3mm
bore that is closed at both ends with uncoated quartz windows. The
dye cell and flashlamp are held in close proximity within a diffusely
reflecting shell. The optical cavity, alignment system and detection
system are the same as those described for the coaxial lamp laser.
Again, no circulation system is used with this arrangement.

Figure 4 shows the adaptation of the ablating flashlamp used to measure the relative fluorescence yields of the dyes.

The following components are designated:

V - Glass or quartz vial

C - Positioning can

F.L. - Ablating flashlamp

R. - Diffuse reflector

F.O. - Fiber optic

′. - Rubber stopper

F - Infrared passing filter

H - Filter holder

D - Photo detector (Tropel #330 Photo Diode)

Equi-molar solutions of potential infrared dyes are exposed to the ablating flashlamp. Any fluorescence is directed by a fiber optics probe through a filter passing only infrared radiation and is detected with a silicon PIN photo diode. Vials of dye solution can be interchanged in a holder adjacent to the flashlamp in a manner that preserves the geometry between probe, detector, and dye sample. Background scattering from pure solvent is subtracted from the readings obtained with the dye.
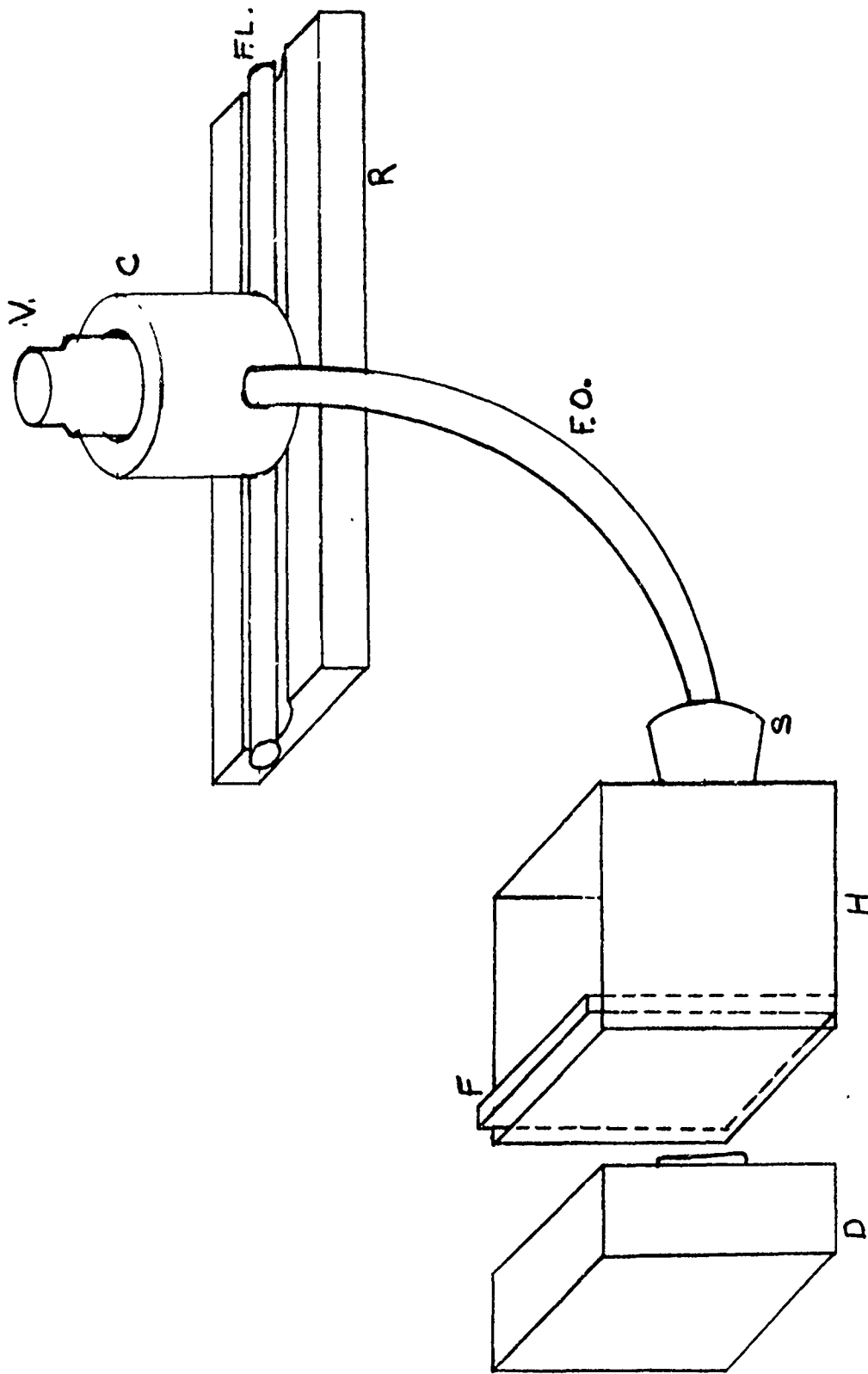
FIGURE 4

Infrared fluorometer employing ablating flashlamp, fiber optics
probe, infrared pass filter, and silicon PIN photo detector.

IV. Test Results

Relative Fluorescence Yield

The infrared fluorescence yields were measured for

the following reasons:

(1) They provide a reliable intercomparison of infrared fluorescence yields between dyes under fast flashlamp excitation at operating dye concentrations. These fluorescence yields provide relative figures of merit comprised of the product of the quantum yield and the efficiency with which flash excitation is coupled the the chromophores of these dyes.

(2) These measurements made on the same dye in several solvents provide information on solvent effects.

Relative fluorescence yields for Kodak dyes AIR-101

through AIR-134 are listed in Table I. The numbers listed are

peak detector output in volts across a 50Ω load, uncorrected for

the spectral sensitivity of the detector. Since the fluorescence

data is not spectrally resolved, a precise correction is impossible.

An approximate correction for detector spectral sensitivity can be

made by assuming the bulk of the fluorescence comes at a wavelength

75 to 100 nm longer than the absorption peak. The spectral sensitivity

of our silicon PIN photo diode appears in Figure 5.

The fluorescence measurements led to the discovery of

dye-solvent combinations that exhibit infrared laser action. Prior

to the fluorescence program, no Kodak dyes had lased in the infrared.

After the fluorescence measurements, the two most promising dye-solvent

29

TABLE I FLUORESCENCE YIELD TESTS

Solvent Test – 10^{-4} M Solutions
Fluorescence Pk – Background Pk. Volts from Tropel 330 Detector

DYE	Methyl Alcohol	Pyridine	$(CH_3)_2SO$ DMSO	$(CH_3)_2NCOH$ DMF	2-Methoxy-Ethanol	Ethyl Alcohol	Propanol
AIR-101	.001	–	–	–	–	–	–
AIR-102	<.001	–	–	–	–	–	–
AIR-103	.006	–	–	–	–	–	.006
AIR-104	–	.008	.004	.003	–	–	–
AIR-105	.012	–	.004	.003	.012	.011	.010
AIR-106	–	<.001	.013	.010	–	–	–
AIR-107	–	.009	–	.008	–	–	–
AIR-108	.001	–	.011	–	–	–	–
AIR-109	.014	–	.027	.023	.018	.014	.013
AIR-110	.01	–	–	–	–	–	–
AIR-111	.1	–	–	–	–	–	–
AIR-112	.16	–	.020	.014	.012	.015	.017
AIR-113	.008	–	.006	.006	.005	–	–
AIR-114	ND	ND	.008	.008	ND	–	ND
AIR-115	.009	–	.008	.009	.007	.014	.006
AIR-116	.015	–	.024	.020	.018	–	.013
AIR-117	.004	–	.004	.004	.014	–	–
AIR-118	.010	.010	.013	.012	.014	–	.020
AIR-119	–	–	–	–	–	–	–
AIR-120	–	.001	–	–	–	–	–
AIR-121	–	–	–	–	.001	–	–
AIR-122	.012	.033	⩽.002	.026	.030	–	.034
AIR-123	–	.013	.039	.013	.010	–	.017
AIR-124	–	–	.015	–	.010	–	.010
AIR-125	.008	–	.016	.013	.010	–	–
AIR-126	<.001	–	<.001	<.001	<.001	.004	–
AIR-127	<.001	–	<.001	<.001	<.001	–	–
AIR-128	<<.001	–	<.001	<<.002	.001	–	–
AIR-129	.001	–	.002	.0022Q	.001	–	–
AIR-130	.003	–	.0025Q .003 .0035Q	.002	.002	–	–
AIR-131	–	–	<<.001	–	<<.001	–	–
AIR-132	.004	.006	.005	.005	.005	–	–
AIR-133	.001•	.002•	.006Q .002 .001•	.002•	.001	–	–
AIR-134	–	.011	.012	.012	.011	–	–
H.F.-4	.009	–	.0135Q	.012	–	–	.008
DTTC	.016	–	.012	.012	.009	–	–
Rhodamine 6G	.19	–	.029	–	–	–	–

– = No data
• = Partially decomposed (visual color change)
ND = Would not dissolve
D = Dye destroyed
Q = Dye solution in quartz cell

30

TABLE I (CONTINUED)

Solvent Test – 10^{-4} M Solutions

Fluorescent Pk – Background Pk.   Volts from Tropel 330 Detector

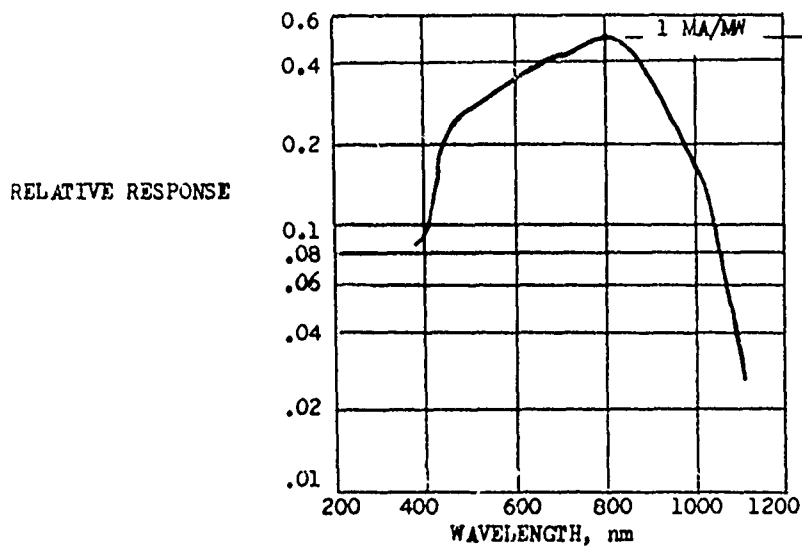| DYE	2,6-Lutidine	Dichloro Methane	Xylene	Dimethyl Acetamide	Hexafluoro Isopropanol	$[(CH_3)_2N]_3PO$ HMPA	Acetone
AIR-101	—	—	—	—	—	—	—
AIR-102	—	—	—	—	—	—	—
AIR-103	—	—	—	—	—	—	—
AIR-104	.013	.008	.014	—	—	—	—
AIR-105	—	—	—	—	—	—	—
AIR-106	—	—	—	—	—	—	—
AIR-107	ND	.004	ND	—	—	—	—
AIR-108	—	—	—	—	D	—	—
AIR-109	—	—	—	—	—	—	—
AIR-110	—	—	—	—	D	—	—
AIR-111	—	—	—	—	—	—	—
AIR-112	—	—	—	—	D	—	—
AIR-113	—	.004	ND	—	—	—	—
AIR-114	—	—	—	—	D	—	—
AIR-115	—	.065	—	—	—	—	—
AIR-116	—	—	—	—	D	—	—
AIR-117	.003	—	—	—	—	—	—
AIR-118	—	—	—	—	—	—	—
AIR-119	—	—	—	.003	—	—	—
AIR-120	—	—	—	—	—	—	—
AIR-121	—	.001	—	< .CC1	—	—	—
AIR-122	.001	.016	—	—	—	—	—
AIR-123	ND	—	ND	—	—	—	—
AIR-124	—	—	—	—	—	.033	—
AIR-125	—	—	—	—	—	.011	—
AIR-126	—	—	—	—	—	.009	—
AIR-127	—	< .001	—	—	—	< .001	< .001
AIR-128	—	—	—	—	—	—	.003
AIR-129	—	—	—	—	—	.001	—
AIR-130	—	—	—	—	—	.003	.002
AIR-131	—	—	—	—	—	.003Q	< .001
AIR-132	—	—	—	—	—	< .001 / .004	.005
AIR-133	—	—	—	—	—	—	.002
AIR-134	—	—	—	—	—	.007	—
H.F.-4	—	.009	—	—	—	—	—
DTC	—	—	—	—	—	—	—
Rhodamine 6G	—	—	—	—	—	—	—

31

RELATIVE RESPONSE

FIGURE 5

Spectral sensitivity of fast silicon PIN photo diode, Tropel
Model 330. The mfrs specified peak sensitivity of 1 amp/watt
is equivalent to 2×10^{-3} amp/watt/cm^2, and agrees with our
(absolute) spectral calibration.

32

pairs of our original 22 candidates (AIR-109 & AIR-116 in DMSO) were immediateiy lased, and one (AIR-107 in DMSO) of the three next most promising dyes lased.

Dye structures of the initial candidates, AIR-101 through AIR-122, were correlated with relative fluorescence yields and lasability. After making these correlations, AIR-123, 124, 125, 129, 130, 132, 133 and 134 were selected for laser testing because their structures looked particularly promising. Six of these eight dyes lased. The structures of AIR-126 and 127 were different from this group; they were tested as part of further exploratory screening. AIR-128 and 131 were related to structurally unpromising dyes. The fluorescence yields from these four dyes were very low.

Perhaps the outstanding result from measuring dye fluorescence is the demonstration of the importance of solvent effects on the emission from these dyes. Fluorescence yields from DTTC, AIR-109 and AIR-116 were almost twice as large in DMSO as in MeOH. These dyes lased in DMSO and failed to lase in MeOH under identical test conditions. Solvent action may be more than simple enhancement of fluorescence. As noted below, a single charge of AIR-109 or AIR-116 in DMSO will put out 4 or 5 substantial, though decreasing, bursts of laser light. After these multiple exposures to the

flashlamp, the dye solutions appear completely bleached. It seems very unlikely that partially bleached dye in DMSO is as fluorescent as fresh dye in MeOH, yet the former still lases while the fresh MeOH solutions will not. The effect of solvent on laser action is not well understood, but we are continuing to study this problem. Hopefully this reporting of our fluorescence yield data will encourage work on solvent effects in other laboratories.

Fluorescence yields of DTTC in 14 solvents are listed in Table II for tests in both glass and quartz vials. While DTTC is not a good laser dye, there is enough dye available to run tests in an extended series of solvents. In these tests ultraviolet pumping seems to have increased infrared fluorescence yields by about 35% compared to the 15% to 20% enhancement shown in Table I for AIR-129, 130, 132, and 134. The greatest fluorescence is produced by DTTC in DMSO.

DMSO seems to be the best solvent for near infrared laser dyes. Since the fluorescence yield as a function of solvent was greatest for DMSO for most dyes, we standardized on DMSO as a solvent for our screening experiments.

We briefly evaluated the relative importance of pumping by infrared light near the primary absorption band of the dye in comparison to pumping across the full flashlamp spectrum. This sort of measurement is an essential prerequisite to future work aimed at improving the coupling efficiency between short wavelength flashlamps and the infrared dyes by using intermediate fluorescent dye solutions

TABLE II

FLUORESCENCE FROM DTTC IODIDE IN SEVERAL SOLVENTS

SOLVENT	*FLUORESCENCE PEAK IN GLASS VIAL (VOLTS)	*FLUORESCENCE PEAK IN QUARTZ VIAL (VOLTS
MeOH	.015	.021
DMSO	.026	.035
DMF	.024	.031
Acetone	.024	.028
HMPA	.019	.023
2 Methoxy EtOH	.017	.027
Ethylene glycol	.024	.031
Dichloromethane	.015	.019
Propanol	.016	.021
Pyridine	.017	.020
Dimethyl Acetamide	.021	.031
2, 6-Lutidine	ND	ND
Glycerol	ND	ND
m-dichlorobenzene	ND	ND

* Voltages normalized to get previously obtained value for DTTC in MeOH, since actual values were 25% low because the flashlamp reflector needed repainting.

ND = DTTC would not dissolve.

as pump frequency down converters. Feasibility of these comparative

measurements was verified for three AIR dyes. In these experiments,

a dye solution was divided between two identical glass vials. One

vial was plain; one had a Wratten #24 filter (transmits wavelengths

longer than 580 nm) taped to the bottom. For AIR-112, AIR-115, and

AIR-118, fluorescence yields from the plain vial were between 2X

and 3X greater than from the filtered vial. While these results

would be more interesting if the dyes had lased, they do show the

importance of broad band pumping as a means for stimulating infrared

fluorescence. The value of short wavelength pumping is due to the

increased output of the flashlamp and the greater absorption band

width at these wavelengths. This technique may be important, since

minor structural features external to the primary chromophore can

aid in absorption of short wavelengths and in transfering this

energy to the infrared fluorescing chromophore.

Infrared Laser Tests

Infrared laser action was demonstrated for nine Kodak dyes

in tests run using the ablating quartz flashlamp. Laser dyes AIR-107,

AIR-109, AIR-116, AIR-123, AIR-125, AIR-129, AIR-130, AIR-132 and AIR-134

(plus Kodak DTTC for comparison) are listed in Table III along with all

of the other candidate dyes. The last four columns of Table III

[lasing wavelength, absolute output power, relative laser output,

and full laser pulse width at half maximum (FWHM)] refer to laser

dyes only. All of the laser data were taken with 10^{-4}M dye

concentrations in DMSO using constant lamp excitation of 128 joules and

the ablating flashlamp, diffuse lamp reflector, and 850-900 nm cavity

mirrors.

TABLE III

SUMMARY OF LASER TESTS

Dye	Relative Fluorescence Yield Peak (Volts)	Solvent	Prior Kodak Data Peak Wavelength nm Abs.	Fluor.	Lasing Wavelength (nm)	Output Power (watts)	Relative Signal Strength of Lasing Dyes $\frac{watt}{cm^2}$	FWHM Nanoseconds
AIR-101	.001	MeOH	--	--	--			
AIR-202	.001	MeOH	--	--	--			
AIR-103	.006	MeOH	803	860	--			
AIR-104	.006	Propanol			--			
	.004	DMSO						
AIR-104	.014	Xylene	650	840	--			
	.014	Lutidine						
AIR-105	.013	DMSO	790	848	NL			
AIR-106	.001	Pyridine	860	950[b]	-			
AIR-107	.011	DMSO	790	940[t]	940	Not Measured	42	210
AIR-108	.001	MeOH	839	860	-			
AIR-109	.027	DMSO	730	832	875	95	100	400[d]
AIR-110	.001	MeOH	-	990[b]	-			
AIR-111	.001	MeOH	855	828	NL			
AIR-112	.020	DMSO	762		-			
	.017	Propanol						
AIR-113	.008	MeOH	766	802	NL			
AIR-114	.008	DMSO	719	780	-			
	.016*	Pyridine						
	.016*	MeOH						
AIR-115	.009	DMSO	765	857	-			
	.009	DMF						
	.009	MeOH						
AIR-116	.024	DMSO	762	830	885	Not Measured	94	400
AIR-117	.004	DMF	810	960[b]	NL			
AIR-118	.004	DMSO	744	830	NL			
	.013	DMSO						
AIR-119	.020	Propanol						
	.003	DMA	788	-	-			
AIR-120	.001	Pyridine	736	742	-			

TABLE III (CONTINUED)

SUMMARY OF LASER TESTS

Dye	Relative Fluorescence Yield Peak (Volts)	Solvent	Prior Kodak Data Peak Wavelength nm — Abs.	Prior Kodak Data Peak Wavelength nm — Fluor.	Lasing Wavelength (nm)	Output Power (watts)	Relative Signal Strength of Lasing Dyes $\frac{watt}{cm^2}$	FWHM Nanoseconds
AIR-121	.001	DMA	715	760	—			
AIR-122	.001	Variety	700/800	745	—			
AIR-123	.0039	DMSO	740	—	850	50	119	400[d]
AIR-124	.015	DMSO	760	—	NL			
	.016	DCM						
AIR-125	.016	DMSO	780	—	940	830	467	500
AIR-126	.001	Variety	815	—	NL			
AIR-127	.001	Variety	780	—	NL			
AIR-128	.001	Variety	730	—	NL			
AIR-129	.0025	Acetone	850	—		Not Measured		
	.002	DMSO			> 930		≳ 370	100
	.0025[Q]	DMSO						
AIR-130	.003	DMSO	805		> 920	Not Measured	≳ 108	150
AIR-131	.0035[Q]	DMSO			NL			
	.001	Variety	970	—				
AIR-132	.0051	DMSO	810	—	960	2kw	1370	500
AIR-133	.006[Q]	DMSO	860	—	NL			
	.0024	Acetone						
	.002[c]	Pyridine						
AIR-134	.012	DMSO	760	—	888	50	44	300
	.0117	DMF						
	.0135[Q]	DMSO						
DTTC	.029	DMSO	760	815	872	Not Measured	24	150

a   Effects of scattering included in data
b   Data uncertain
d   Saturated detector
Q   Quartzcell for containing solution
c   Decomposition (visible change in color)
NL   Did not lase
—   Not tested in laser facility because of low fluorescence yield

Lasing wavelength was reported as the center wavelength
of the spectrograms which were often exposed by several laser pulses.
The apparent spectral width of laser emission is not listed as it depends
so strongly on exposure and film sensitivity at the lasing wavelength.
No densitometer curves were run on the spectrograms to determine
spectral FWHM of the outputs; apparent total width to the extreme
wings was 5 to 10 nm.

Absolute laser output power was measured using the
following apparatus and calculation. An opal glass target of 4mm
thickness was positioned at a distance R = 9 cm in front of a
calibrated silicon photo diode with photo sensitive area
$dS_d = 2 \times 10^{-3} cm^2$. Assuming the opal glass target is a perfect
diffuser, $\frac{d\Omega}{4\pi} = dS_d/4\pi R^2 = 2 \times 10^{-6}$. Only this small amount
of the laser light incident on the target reaches the detector.
The peak laser output power is estimated as

$$J_o \text{ (watt)} = \frac{4\pi}{d\Omega} \frac{\text{Sig. (amp)}}{S \left(\frac{amp}{watts}\right)} \tag{7}$$

where J_o is the peak laser power, Sig is detector photo current, and
S is the spectral sensitivity of the photo detector. Output power
was determined only for the most energetic laser dyes because of the
low detector signal after the diffuser attenuation.

Relative signal strengths were measured by placing the
photo diode directly on the dye laser axis about 1 meter from the
dye cell. The signal is measured in watt/cm^2 and is corrected to

include the effect of any neutral density filters and the spectral sensitivity of the detector when the laser wavelength is known. The lasing wavelengths of AIR-129 and AIR-130 have not been determined, because of low film sensitivity in the spectrograph at long wavelengths. Based on dye absorptions, their lasing wavelengths are probably longer than the listed minimum values. Hence, relative output signals are underestimated because detector sensitivity is decreasing with wavelength past 920 nm.

Relative output signals give a qualitative comparison of laser output power between energetic dyes whose absolute output was measured and dyes such as DTTC whose output could not be measured with the diffuser. Note that the very small active area of the detector was almost certainly probing different parts of the output beam during experiments on different laser dyes. This uncertainty is added to other discussed in Section V and leads to only qualitative usefulness for the measured signal strengths.

Measurements of laser pulse duration (FWHM) were derived from oscilloscope photos taken with the detector on axis. The longest pulse duration ($\sim$ 500 ns) for AIR-125 and AIR-132 should be compared with pulses of $\sim$ 700 ns for rhodamine 6G in DMSO. The rhodamine laser measurement was also made at 128 joules, but with infrared reflecting mirrors which are not optimum for rhodamine. Peak

rhodamine 6G laser output on this 700 ns pulse was 2.7 kw versus
∿ 0.8 kw and 2 kw for 500 ns pulses from AIR-125 and AIR-132,
respectively. Other less energetic AIR dyes displayed shorter
pulse widths.

Stability of the laser dye solutions under intense,
ultraviolet rich excitation from the flashlamp was investigated
by repetitively lasing the same ∿ 2 cm^3 charge of dye solution,
and monitoring the output. Peak outputs from such repetitive shots
on single charges of AIR dyes are listed in Table IV. Data for
AIR-129 is omitted because changes in the equipment prevented
repeated lasing of AIR-129. A similar test was run on rhodamine
6G in DMSO. The first shot saturated the detector at 96 volts;
the second shot barely lased (visually) and would not trigger
the oscilloscope (trigger level at 10 volts). The third shot
did not lase visually and failed to trigger the scope at 1 volt
triggering level. Based on this comparison with a stable
xanthene dye, dyes such as AIR-132, AIR-125 and probably AIR-109
and AIR-123 withstand flashlamp pumping better than would be
expected for such large, non-rigid molecules. Dye degradation does
exist, but repetitive laser action is possible from the same small
charge of dye solution, indicating that the production of long-lived
photo bi-products that absorb at the lasing wavelength must
be very small. Incidentally, this test is particularly sensitive

TABLE IV

DYE STABILITY TEST

PEAK VOLTAGE FROM DYE LASER PULSES

Flash Number / Dye	1	2	3	4	5	6	7	8	9	10	11
DTTC	1.0	2.0	1.5	1.0	0.6	.14	NT	-	-	-	-
AIR-107	2.0	NT	-	-	-	-	-	-	-	-	-
AIR-109	8.0	7.0	9.2	4.4	2.0	2.2	NT	-	-	-	-
AIR-116	8.2	3.6	4.5	4.0	2.2	0.5	NT	-	-	-	-
AIR-123	11.0	10.0	10.0	NT	-	-	-	-	-	-	-
AIR-125	11.0S	9.0	6.4	>10.0	6.6	10.0	7.0	5.0	NT	-	-
AIR-130	7.0	0.04	NT	-	-	-	-	-	-	-	-
AIR-132	12.5S	12.5	9.0	6.4	6.4	2.0	1.4	1.2	1.2	0.6	-
AIR-134	3.7	2.6	0.6	0.23	0.18	0.025	-	-	-	-	-

NOTES:

> indicates trace went off scale
NT means the signal would not trigger the oscilloscope
- no data taken
S detector saturated

TEST CONDITIONS: 10^{-4} M concentration for all dyes in DMSO; non-circulating dye solution, 5-10 minute wait between shots; 850-900 nm mirrors; $R_1 = R_2 = 98\% \pm 1\%$; energy input per flash is 128 joules at 16,000 volts

DETECTOR: Tropel, Model 330 pin photo diode, looking at laser axis.

42

for AIR-132, since it has a low fluorescence yield (proportional to $n^*\sigma_g$) and a low gain; thus, continued laser action would be quenched by any substantial increase in loss factors.

Representative oscilloscope traces from all of the infrared laser dyes are included in Figure 6. All signals were recorded with the detector on axis, screened by an infrared pass filter, and sometimes by an Inconel 0.9 ND filter. Non-circulating dye solutions were all 10^{-4}M concentration in DMSO, the ablating quartz lamp input was a constant 128 joules, and the mirrors reflecting at 850 to 900 nm were used throughout.

FIGURE 6

Laser output of flashlamp pumped infrared dyes. Detector sensitivity
varied from ∿ 0.05 V/watt/cm² at 960 nm to ∿ 0.09 V/watt/cm² at 850 nm.
See text for other test conditions.
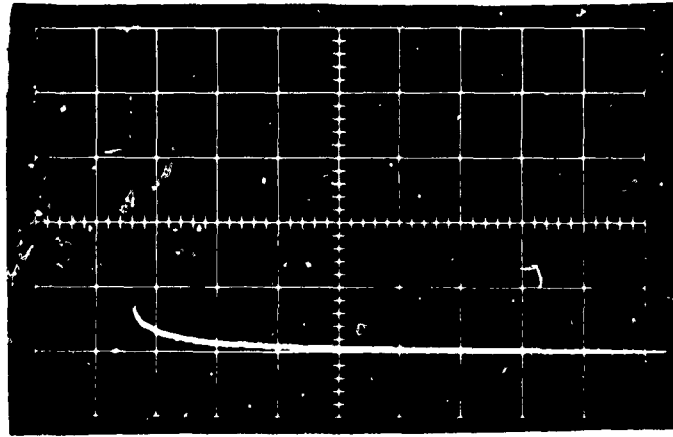
(a)   AIR-107 - 10^{-4}M in DMSO; 0.5 volt/div;
      1 μsec/div
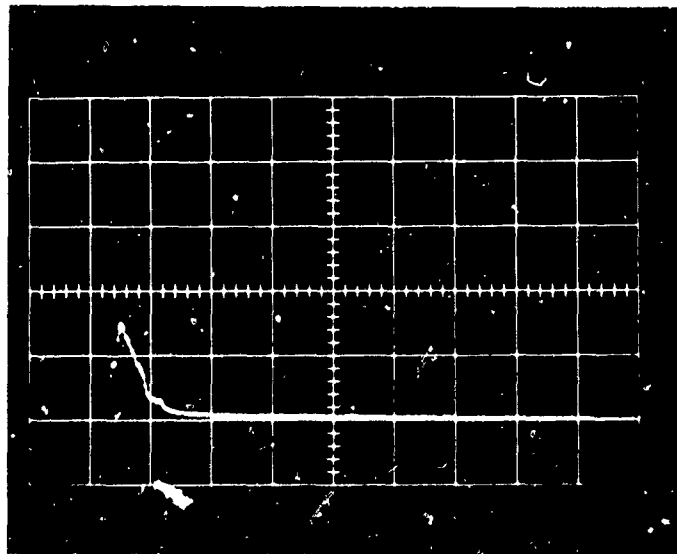
(b)   AIR-109 - 10^{-4}M in DMSO; 5 volt/div;
      1 μsec/div
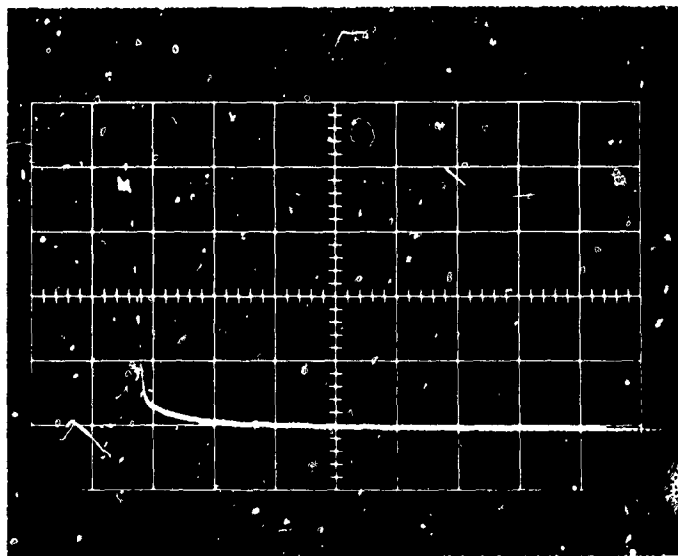
FIGURE 6 (CONTINUED)

(c)   AIR-116 - 10^{-4}M in DMSO; 2 volt/div;
      1 μsec/aiv
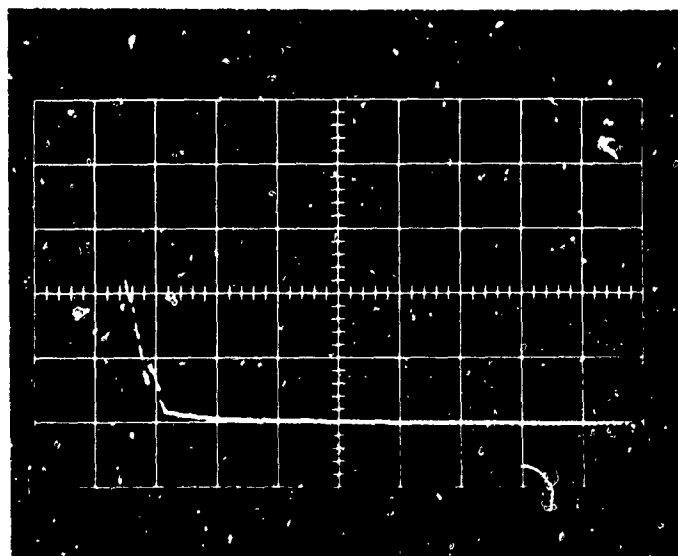
(d)   AIR-123 - 10^{-4}M in DMSO; 5 volt/div;
      1 μsec/div
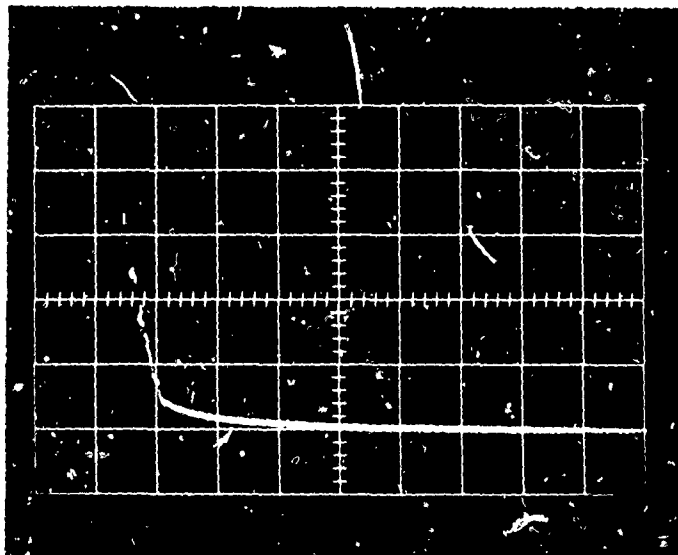
FIGURE 6 (CONTINUED)

(e)   AIR-125 - 10^{-4}M in DMSO; 0.9 ND Filter
on Axis; 1 volt/div; 1 μsec/div
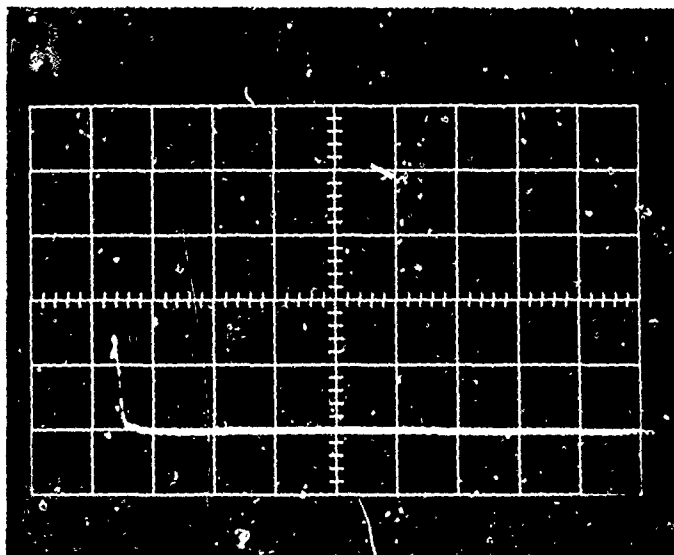
(f)   AIR-129 - 10^{-4}M in DMSO; 0.9 ND Filter
on Axis; 2 volt/div; 1 μsec/div

46
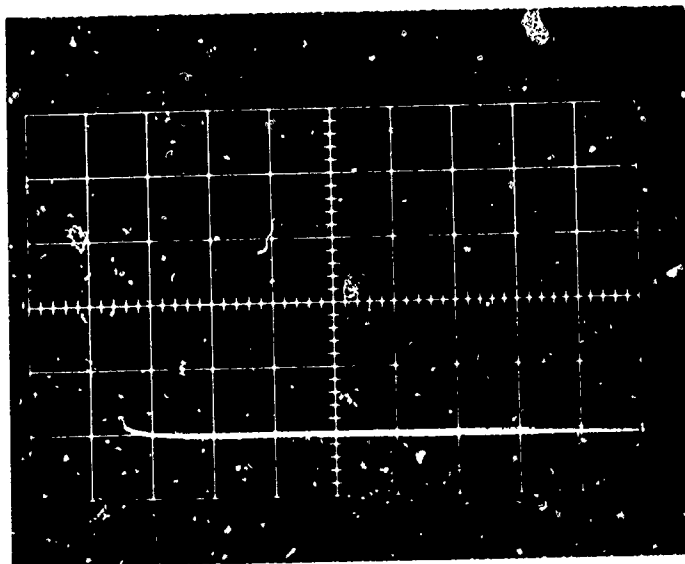
FIGURE 6 (CONTINUED)

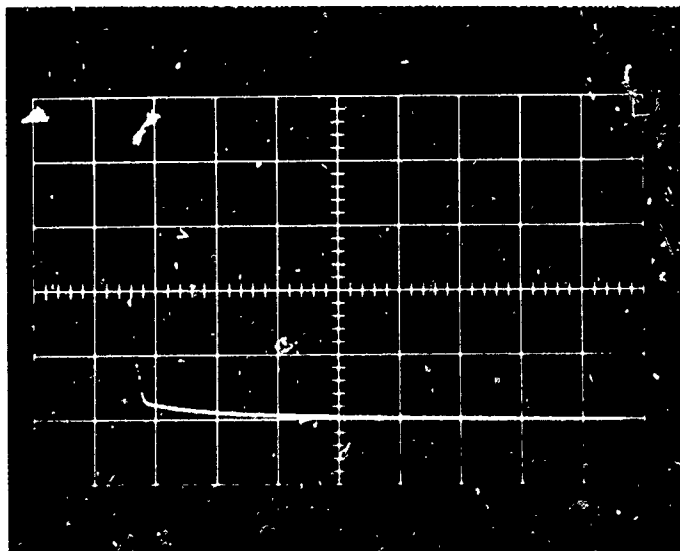(g) AIR-130 - 10^{-4}M in DMSO; 2 volt/div;
1 µsec/div
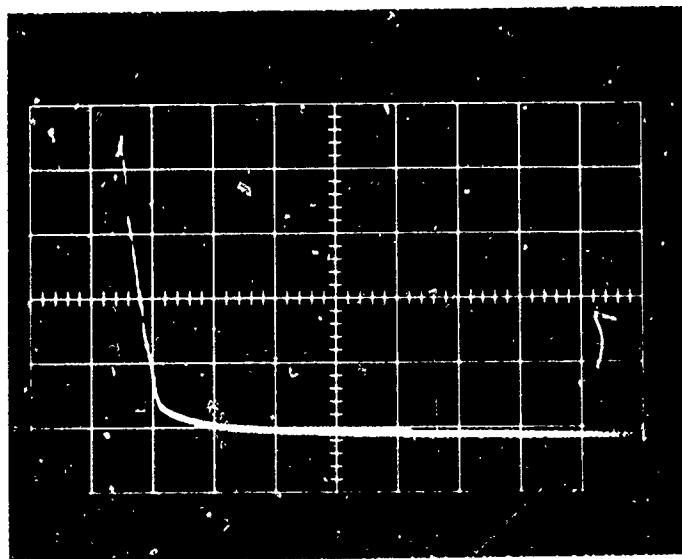
(h) AIR-132 - 10^{-4}M in DMSO; 0.9 ND Filter
on Axis; 2 volt/div; 1 µsec/div

FIGURE 6 (CONTINUED)
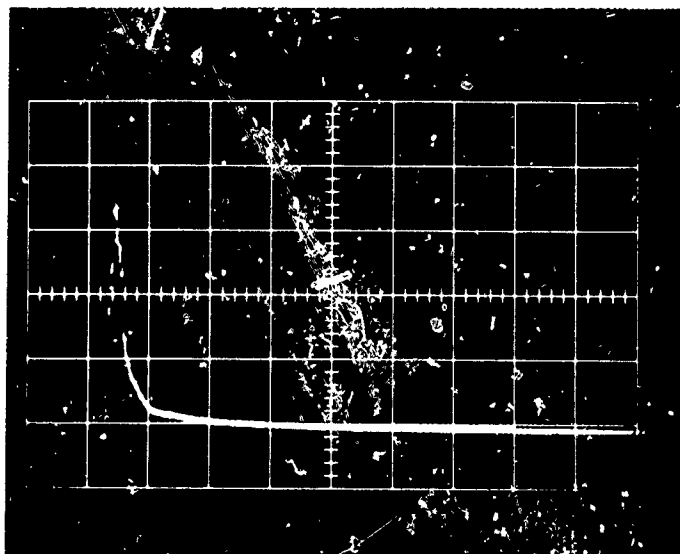
(i) AIR-134 - 10^{-4}M in DMSO; 1 volt/div;
     1 μsec/div

(j) DTTC-Iodide - 10^{-4}M in DMSO;
     1 volt/div; 1 μsec/div

V. Difficulties and Limitations

Difficulties encountered in this work were either fundamental limitations inherent in flashlamp pumping infrared dye lasers or experimental problems peculiar to this dye screening program.

The main fundamental limitation to flashlamp pumped infrared dye lasers is the low fluorescence yield of these dyes when excited by a flashlamp emitting short wavelengths. Figure 7 plots as a function of the wavelength of their absorption maxima the peak fluorescence yields of several laser dyes excited by our ablating flashlamp. Rhodamine 6G was measured in MeOH; the other fluorescence yields were all determined in DMSO. Some of this low yield almost certainly results from the lower quantum yields of these large dye molecules. The quantum yield of DTTC in methanol, for example, has been measured as 15% by L. F. Costa of the Kodak Research Laboratories (8), as compared with a reported value of 85% for rhodamine 6G (6). Assuming that the quantum and fluorescence yields depend identically on solvents, this difference would predict a quantum yield for DTTC in DMSO of ~ 30%, or about one-third the quantum yield of rhodamine 6G. The fluorescence yield of DTTC in DMSO is lower by an order of magnitude than that for rhodamine, however. This discrepancy is attributed to a better

(6) O. Peterson, J. Webb, W. McColgin and J. Eberly,
    J. A. P. 42, 1917 (1971).
(8) L. Costa, Kodak Research Laboratories (private communication).
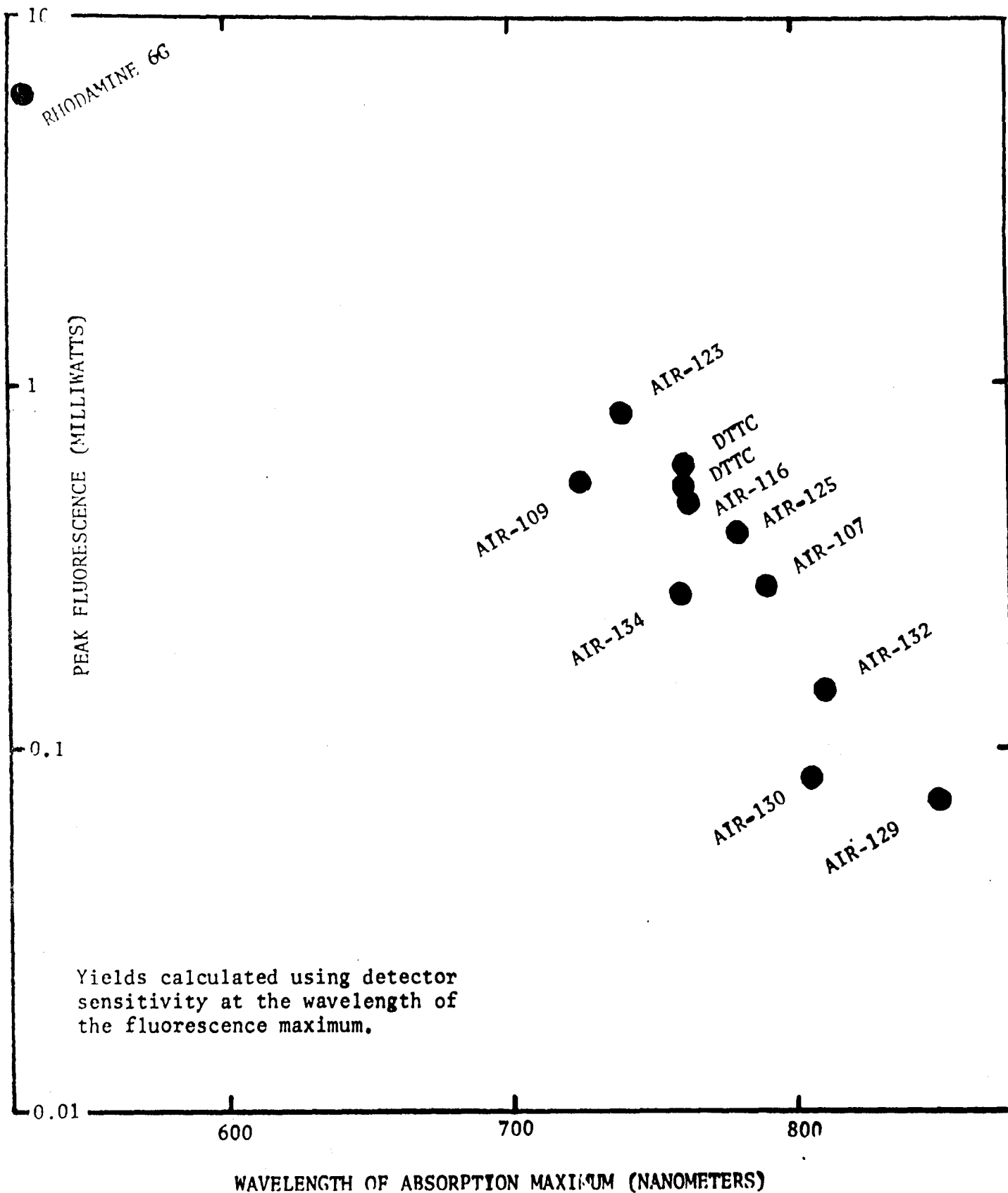
WAVELENGTH OF ABSORPTION MAXIMUM (NANOMETERS)

FIGURE 7

Relative infrared fluorescence yields of
laser dyes as a function of wavelength of
the dyes' absorption maxima. Fluorescence
yields were measured on the fluorometer
with the same geometry between dye and
detector for all tests.

50

spectral overlap between the flashlamp excitation and the absorption

bands for a visible dye. The poor spectral overlap for infrared dyes

is a second part of this fundamental problem. The rapid dissipation

of energy in the flash required to produce an intense enough excitation

to pump n^+/n to threshold inversion also produces a high color

temperature plasma. This source approximates a black body radiator

whose spectral output is strongly peaked in the ultraviolet.

The strong dependence of fluorescence yields on solvent

mandates further solvent effect research. Unfortunately, solvents

like DMSO and ethylene glycol that best enhance fluorescence lack of

desirable flow and schlieren properties of the lower alcohols and

water, and thus may increase extrinsic losses in a laser with a

circulating dye solution.

Fortunately, the limitations of dye stability and triplet

state buildup with attendant triplet-triplet absorption proved less

severe than anticipated, at least with the better AIR dyes. Problems

associated with these phenomena will always exist, however, and thus

will warrant continued attention.

All of these dyes are unstable in solution and require

special handling. We always worked in subdued tungsten light and

refrigerated the dye solutions over night. Under these conditions,

dye solutions could be used for many days, and refrigerated samples

lasted for weeks or months. We mixed only 10 or 20 cm^3 samples at

51

a time and always exhausted the solution before degradation appeared.
Since DMSO freezes at 18°C, refrigerated samples had to be thawed
each morning, a procedure that may become time consuming if
liter-sized volumes are prepared for a later generation flow-system.

Our most serious experimental difficulties were caused
by the very limited quantities of these experimental dyes. In this
work we have minimized the volume of dye solution by using only
enough to fill the cell itself, syringing rinse and dye solutions
in and out of the cell for each test. Thermal equilibration was
accomplished by waiting about 10 minutes between tests.

This test procedure was slow and the single shot mode
of operation was deleterious in more subtle ways. For example,
adjusting the system by measuring successive laser outputs while
making minor changes in alignment was difficult. There was not
enough dye, and during the alignment series, temperature drifts
would occur more rapidly than we could compensate for them.
Laser output was degraded by a slow darkening of the diffuse
reflector surrounding lamp and dye cell or a gradual spotting
that appeared on the inside of the windows. It is difficult to
separate minor alignment degradation from this irreversible
degradation.

52

We switched to the ablating lamp and small ID quartz cell after we could not get laser action using the Candela coaxial lamps. These new cells, one of which is illustrated in Figure 8d, were hastily constructed in our glass shop. Uncoated end windows were attached with RTV-silicone rubber (D.C.-731), which is compatible with dyes in many solvents including pyridine which attacks most epoxies. Gluing was done without a precision jig, and the cell bodies were used as cut on a diamond wheel with no subsequent grinding. Because of nonuniform glue thickness and nonparallel ends of the cell body, the windows were neither parallel to each other nor perpendicular to the cell axis. The filled cell was a skewed prism with a usable volume 144mm long and 3mm in diameter. Initial alignment of the resonant cavity containing this elongated skewed prism was difficult. In addition, the prismaticity of the cell appeared to change in time. We attribute these changes to variable swelling of different portions of the nonuniform silicone rubber adhesive layer, and perhaps to solvent impurity or temperature induced variations in the index of refraction of the solution.
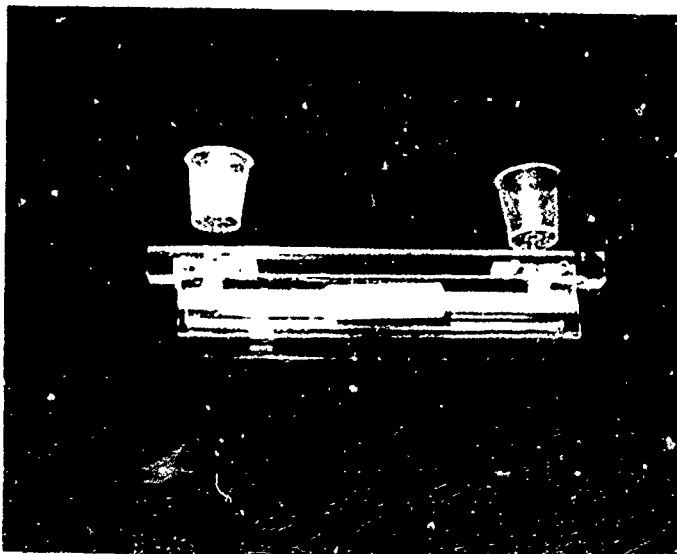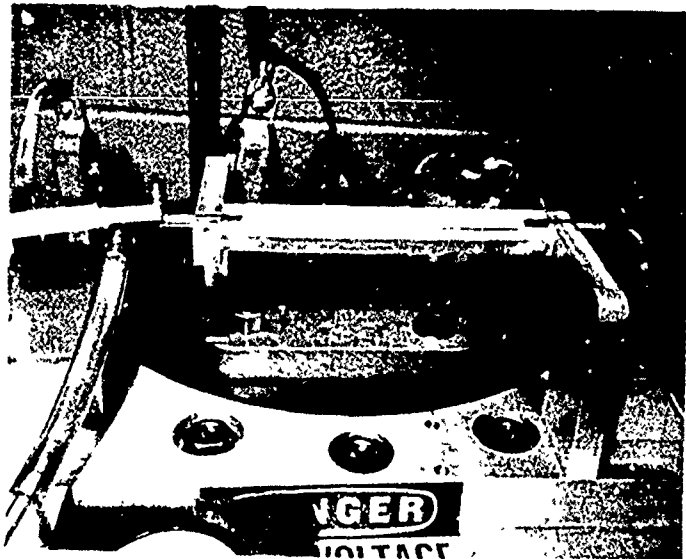
FIGURE 8

DYE LASER
SCREENING
FACILITY
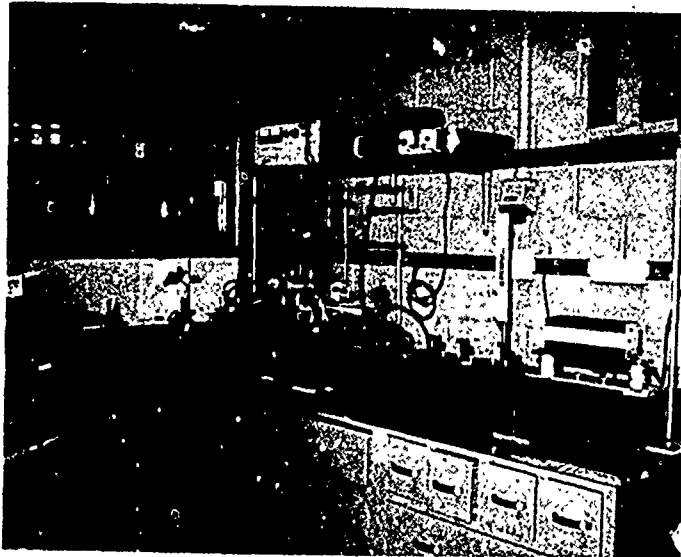
(a) View of test facility showing
spectrograph behind oscilloscope
at left, optical bench with
beam steering mirrors and prisms,
filter holders, target and detector,
He-Ne alignment laser at right, and
dye laser mounted on 1 µfarad
capacitor in center.

ABLATING FLASH LAMP

(b) Ablating flashlamp located
between electrode-bus supports,
and positioned in bottom half of
split, diffuse reflector.

DYE CELL IN HOLDER

(c) Laser dye cell in holder with
top half of split, diffuse
reflector. The machined holder
can be removed and reproducibly
repositioned on the bottom half
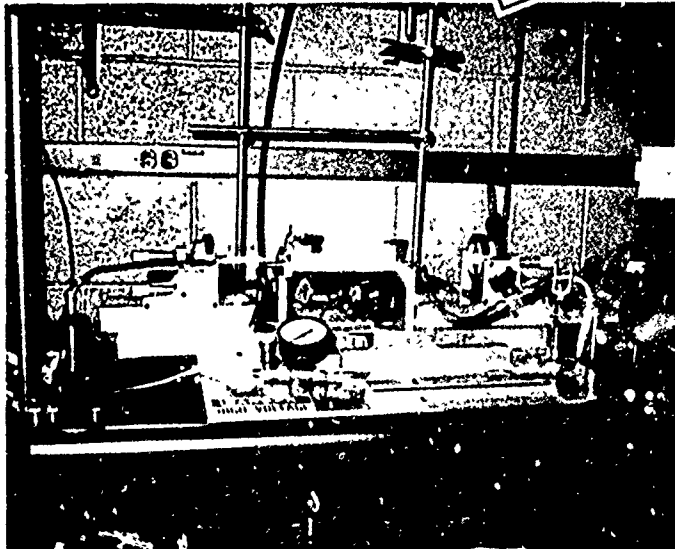of the split reflector.

FIGURE 8 (CONTINUED)
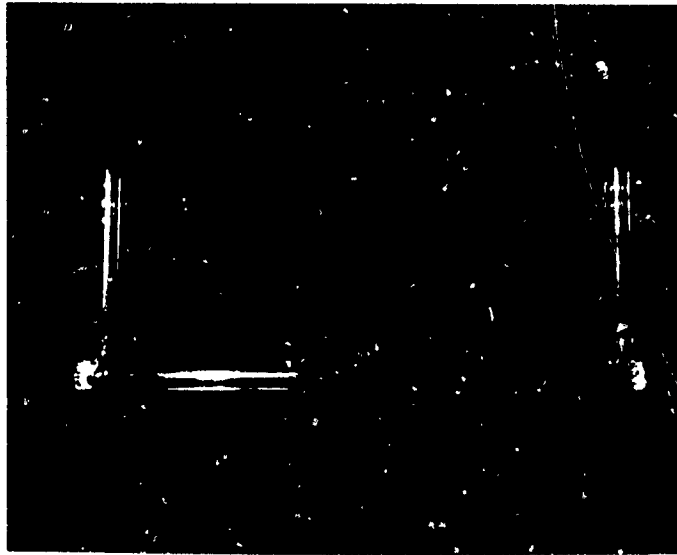
DYE CELL

(d)   Three mm ID laser dye cell.

CLOSE UP OF DYE LASER

(e) Close-up of dye laser showing cavity mirrors, diffuse reflector housing containing
flashlamp and dye cell between electrode-bus supports, flashlamp pump hose to vacuum
pump at right, and flashlamp trigger hose and needle valve at left. The laser is
mounted on top of a 1 µfarad drum capacitor adjacent to the optical bench.

VI. Conclusions

The following conclusions are drawn from these tests:

1.) AIR-132 and AIR-125 are the two most promising laser dyes. Both lase around 850 nm, and have outputs in the kilowatt range. AIR-109 and AIR-123 are less promising, ($\sim$ 0.1 kw outputs), but do lase in the 850 to 875 nm range.

2.) AIR-132, AIR-129, AIR-130, and AIR-134 are particularly interesting laser dyes because of their low fluorescence yields relative to other infrared laser dyes. Recall that these fluorescence yields are proportional to the product of the dyes' quantum yield and the excited state population n* excited by the flashlamp. The gain of a dye is proportional to $n^*\sigma_g(\nu)$, and thus the good laser action of these dyes relative to their low fluorescence yields might be explained in two ways:

   a) The fluorescence line shape $g(\nu)$ is sharper, and hence higher at λ_{lase} than for other infrared laser dyes, thus increasing $\sigma_g(\nu) = c^2 g(\nu)/8\pi\, \nu^2\, \tau_S\, n^2$ over the $n^* \int g(\nu)\, d\nu/\tau_S n^3$ value reflected in the quantum yield. The ν^{-2} term clearly increases σ_g for these long wavelength laser dyes, but scarcely by enough to compensate for the reduced fluorescence yield.

   b) These are particularly low loss dyes, i.e. $\sigma_g(\nu)$ is relatively larger than $\sigma_s(\nu)$, $\sigma_{ss}(\nu)$ and $\sigma_T(\nu)$ at the lasing wavelength. In fact, these dyes do seem to lase at wavelengths further removed from their absorption maxima than dyes of different families such as DTTC, AIR-116, and AIR-123. (AIR-109 is related to AIR-132, etc., and even AIR-107 has some structural similarity. AIR-125 is the only dye related to this group that has a comparable shift from absorption maximum to lasing wavelength. The low-loss theory is favored by the fact that AIR-129 refused to lase at all in later tests when the laser test facility had higher extrinsic loss. Under identical circumstances, AIR-132 lased at only 22% of previous peak outputs (versus DTTC lasing at 50% of previous peaks), a result also supporting the low loss hypothesis. In this case increased extrinsic loss is substituted for the low intrinsic loss of AIR-129 and 132 to quench laser action.

The important task of unraveling what makes dyes of this class good laser dyes requires an accurate spectral analysis of fluorescence. Understanding what structural features make a good infrared laser dye is crucial to any future effort to enhance laser performance through molecular engineering. At the moment we lack a firm understanding in this area.

3.) The low fluorescence yield of long wavelength dyes (AIR-107, 129, 130, and 132) is tentatively attributed to poor spectral overlap between the short wavelength flashlamp and the infrared absorbing dyes. Low efficiency pumping leads to lower excited state populations n^* in the dyes. Figure 7 shows the peak fluorescence yields of several laser dyes excited by the ablating lamp and measured at the end of the fiber optics probe of our fluorometer. The peak fluorescence yields are corrected for the spectral sensitivity of the detector and are plotted against the wavelength of the absorption maximum of the dyes. Rhodamine 6G was in MeOH; all other dyes were in DMSO.

4.) Infrared dye stability appears good under intense flashlamp excitation compared to that of rhodamine 6G.

5.) The measured laser pulse duration suggests that triplet buildup is not a serious problem with the better AIR dyes. Further investigation of this point is needed.

VII. Recommended Future Work

Further research is needed to optimize a dye laser system. We must secure enough dye to set up and operate a flow system and obtain reproducible data. Experimental variability and long-term degradation must be understood and reduced or eliminated.

The goals of this work are a better understanding of the physics and chemistry of the components of a flashlamp pumped infrared dye laser system and the enhancement of laser output and efficiency. A two-pronged effort is recommended:

A. Physical/Engineering Investigation and Enhancement

1) Set up a reliable flow test system that would permit acquisition of reproducible laser data at a reasonable rate. Find pumps and components compatible with laser dye solvents. Make better cells that eliminate prismaticity, have coated end plates, and allow cleaning of the insides of the windows. Try a blue alignment laser (He-Cd) to probe optical homogeneity since 6328Å light is too strongly absorbed to be a useful probe.

2) Optimize the system configuration by varying mirror reflectivities, cavity size, cell shape, dye concentration, and excitation energies.

3) Measure laser thresholds and slope efficiencies as soon as reproducible data are obtained.

58

4) Investigate different excitation schemes to improve pumping efficiency and spectral overlap. A high speed, linear xenon flashlamp should be substituted for the air-discharge, ablating lamp. Xenon converts input energy into light more efficiently than air (9), and might emit more red light. Try to convert blue-rich flashlamp radiation using the Stokes shift of intermediate fluorescent dyes. From knowledge of pumping efficiency as a function of excitation wavelength try to shield the infrared dyes from destructive short wavelengths and thus enhance dye stability. Search for an intermediate dye that would absorb in a pumping window and fluoresce in the absorption band of an AIR dye.

B. Chemical Investigations and Enhancement

1) Continue screening of new potential laser dyes based on the information correlating dye structures with lasability derived in this work.

2) Investigate solvent effects in order to correlate solvent structure with fluorescence yield and lasability.

3) Determine what stops laser action. Triplet buildup with attendant triplet-triplet absorption, dye degradation, thermally and acoustically-induced inhomogeneities, and simple termination of the flash could cause quenching of laser action. For this work equipment is needed to simultaneously monitor excitation intensity, laser output, and solution homogeneity.

(9) R. Panico, Xenon Corp. (private communication).